Determining the Impact of the Different Losses on Centrifugal Compressor Design

Barend W. Botha and Adriaan Moolman*

The use of computational performance prediction methods has led to significant improvement in turbo-machine technology. One important aspect in this process is the correct simulation of the various losses. This led to previous studies deducting mathematical models for the losses. This study briefly summarises these loss models. Thereafter it presents the results of a parametric study as to the effect of each type of loss mechanism on the performance at both design and off-design conditions. This can aid the designer in justifying design decisions which could impact on minimising the magnitude of the losses and thus positively influence the overall performance.

Introduction

The increased use of computational performance prediction methods to aid in the design process has led to a significant improvement in turbo-machine technology over the past few years. Using these useful simulation capabilities, together with a good understanding of the mechanisms affecting the performance, can aid in eliminating trial-and-error type design processes. One such a mechanism having a significant impact on performance prediction is the different loss mechanisms experienced throughout the compressor. In order to improve a specific compressor design for an application in a different operating condition, it is important to understand the influence of the various loss mechanisms on the performance of the unit. This will aid the designer in reducing the most important losses to improve compressor performance at specified conditions.

Various studies in the past have concentrated on identifying the different loss mechanisms and developing suitable models to aid in predicting centrifugal compressor performance more accurately. Some of the more important studies include the work of Jansen[1], Whitfield & Baines[2] and Aungier[3]. Following this, Oh et al.[4] performed a detailed study comparing the different loss models presented in open literature and suggested a set of loss models accurately predicting the performance of a number of different impeller configurations. Based on the models suggested by Oh et al.[4], the present study investigates the effects of the different loss mechanisms on the performance of centrifugal compressors at different operating conditions. Finally, the results of a detailed parametric study (performed on a small scale turbo-charger type centrifugal compressor) are discussed after which the most important loss mechanisms are identified for different operating conditions. Although Japikse[14] states that two-zone modelling is a more accurate performance prediction method, this method requires a great deal of experience in compressor performance prediction and design. Therefore, this study purposefully uses the single zone loss model approach, in order to allow the inexperienced design engineer or simulation engineer to become more acquainted with important performance prediction and design aspects. It should be noted that Reynolds number effects are not taken into account in the parametric studies, and care should be taken when applying the results directly towards larger sized impellers.

*Senior Lecturer, School of Mechanical and Materials Engineering, Potchefstroom Campus, North-West University, South Africa
Email: mgibwb@puk.ac.za

NOMENCLATURE

b	Impeller width
b^*	Ratio of vaneless diffuser inlet width to impeller exit width
C_p	Specific heat at constant pressure
C_f	Skin friction coefficient
d	Diameter
f	Loss coefficient
h	Enthalpy
i	Incidence angle
L_b	Impeller flow length
L_θ	Impeller meridional length
$\dot{m}$	Mass flow rate
P	Pressure
PR	Pressure ratio
r	Radius
T	Temperature
U	Tangential impeller speed
V	Absolute velocity
W	Relative velocity
W_{ui}	Tangential difference between ideal and actual relative inlet flow
W_x	Total shaft work per unit mass flow
Z	Number of blades
α	Absolute flow angle from meridional direction
β	Relative flow angle from meridional direction
x	Wake mass flow fraction
ε	Wake fraction of blade-to-blade space
ε_c	Clearance gap
γ	Specific heat ratio
η	Efficiency
ρ	Density
ω	Rotational speed

Subscripts

0	Total or stagnation flow conditions
1	Impeller inlet
2	Impeller exit and vaneless diffuser inlet
3	Vaneless diffuser exit
bld	Blade loading
cl	Clearance
df	Disc friction
h	Impeller inlet hub location
hyd	Hydraulic
inc	Incidence
j	Jet zone
lk	Leakage
m	Meridional direction; mixed-out state
mix	Mixing

rc Recirculation
s Shroud
sf Skin friction
vld Vaneless diffuser
w Wake zone
θ Tangential direction

Loss Mechanisms

The loss mechanisms found in centrifugal turbo machines which negatively affect the efficiency can be divided into two main groups, i.e. (1) internal loss mechanisms and (2) parasitic loss mechanisms.

Internal loss mechanisms are associated with losses emanating from the main flow through the compressor, thereby affecting the efficiency as well as the pressure ratio of the compressor. These include the incidence loss at impeller entry, the three main groups for the flow through the impeller i.e. the blade loading loss, skin friction loss and clearance loss and the mixing loss at the impeller exit. In contrast, parasitic loss mechanisms are associated with losses emanating from minor flows leaking away from the main flow through the compressor. In addition to the internal losses, the parasitic losses give rise to an increase in impeller discharge stagnation enthalpy without any corresponding change in pressure. This means that the compressor efficiency is reduced without any effect on the pressure ratio. The main parasitic losses include the (1) disc friction loss, (2) recirculation loss and (3) leakage loss. Figure 1 illustrates where these different parasitic losses occur.

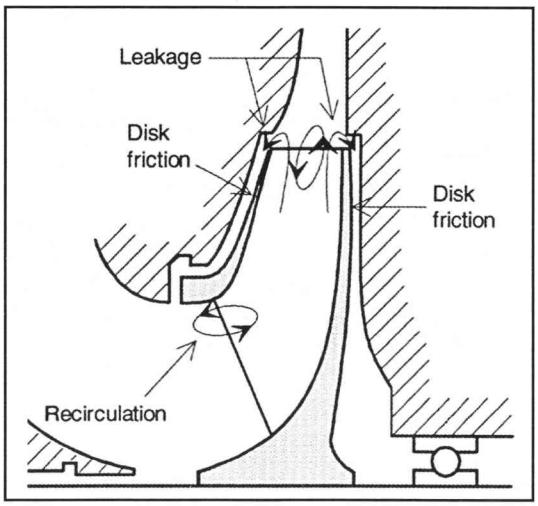

Figure 1: Parasitic Losses (Adapted from Japikse and Baines[8])

Loss Models

Oh et al.[4] performed a detailed study comparing the different loss models describing the mentioned mechanisms as presented in open literature. These models are briefly discussed before presenting the results of the detailed parametric study.

Incidence loss

The incidence loss occurs when the relative fluid flow angle of the fluid entering the impeller deviates from the actual blade inlet angle. This means that the fluid has to change direction immediately, resulting in a significant loss in energy. The closer the blade angle is to the relative flow angle, the smoother the transfer and the lower the loss. In early designs, the blading was made up of simple straight-line elements not necessarily aligned to represent the relative flow field at the inlet. This resulted in very high losses occurring and, over time, led to designs changing to blades being curved in the direction of the entering flow (relative flow) to control incidence levels. This initial part of the impeller is called the inducer and can, if well-designed, improve stage performance.

Oh et al.[4] suggested that the model of Conrad et al.[10] yielded the most accurate results for the incidence loss. According to the latter, the vanes determine the mean surface flow in the inducer section. The change in momentum due to the blade thickness and the deflection in the direction of the blades results in a loss of energy causing the so called incidence loss. According to Oh, the most applicable model is subsequently given by

$$\Delta h_{inc} = f_{inc}\frac{W_{ui}^2}{2} \quad (1)$$

where Δh_{inc} is the enthalpy loss and f_{inc} is the energy loss coefficient which must be determined experimentally, but in the case where experimental correlations are unavailable, Conrad et al.[10] suggests using a value of 0.5 to 0.7.

Blade loading loss

Jansen[1] describes the blade loading loss as the momentum loss due to boundary-layer build-up on the blade surfaces and provides the following loss model:

$$\Delta h_{bld} = 0.05 D_f^2 U_2^2 \quad (2)$$

This shows the blade loading loss to be a function of the diffusion factor D_f squared and the tangential impeller speed U_2 squared. D_f provides a quantitative measure of the total diffusion (deceleration of flow) in the impeller passage and U is the tangential velocity or the circumferential speed at the impeller exit. *Df*, in turn, can be determined by:

$$D_f = 1 - \frac{W_2}{W_{1s}} + \frac{0.75\Delta h_{Euler}/U_2^2}{(W_{1s}/W_2)\left[(Z/\pi)(1-d_{1s}/d_2)+2d_{1s}/d_2\right]} \quad (3)$$

The first section of Equation (3) is related to the diffusion of the flow passage in the form of a decrease in average velocity through the passage. The second part is related to the loading distribution on the blade. This will normally cause an increase in the blade surface velocity at the impeller inlet. This means that the diffusion factor is a function of the one-dimensional deceleration and turning of the flow.

From the above equations it can be deduced that changing the relative flows (inlet and exit) and the tangential impeller exit speed will result in a change in blade loading loss.

Skin friction loss

According to Jansen[1] the skin friction loss is the loss experienced due to the adhesive forces between the channel surfaces and the fluid. The channel surfaces are those surfaces created by the hub, blades and shroud. It is assumed to be equivalent to that experienced by a fully developed flow in a pipe of circular cross-section, with a diameter and length equal to the average hydraulic diameter and the average length of the impeller flow passage respectively, provided in Jansen[1]. This loss specifically excludes the effect of the non-uniform velocity distribution caused by the work addition process in the impeller on the blade surface due to the boundary-layer behaviour. The suggested model for calculating the mass-averaged loss is given as

$$\Delta h_{sf} = 2C_f \frac{L_b}{d_{hyd}} \bar{W}^2 \quad (4)$$

where $\bar{W} = \frac{V_{1s} + V_2 + W_{1s} + 2W_{1h} + 3W_2}{8}$ is given by Oh et al.[4] as the mean relative velocity in the impeller passage.

Clearance loss

In order to allow free rotation, a finite clearance gap is essential between the impeller and the stationary casing. In the case of commonly used unshrouded impellers, fluid will leak through this gap (between the blade tip and casing) from the higher pressure on the pressure side of the blade to the lower pressure on the suction side of the blade. This mixing of the two flows results in the so-called clearance loss in the form of a small vortex on the suction side (low pressure region) of the impeller vane outer tip. Jansen[1] explains how this leakage flow undergoes a sudden contraction followed by a sudden expansion across the clearance gap. This affects both the leakage flow and the main stream into which it discharges. A characteristic blade loading is assumed to estimate the pressure difference acting across the clearance gap. The total pressure losses are obtained by assigning standard loss factors to the sudden contraction and sudden expansion processes. This results in the following clearance loss model given by Jansen[1]:

$$\Delta h_{cl} = 0.6 \frac{\varepsilon_c}{b_2} V_{\theta 2} \left\{ \frac{4\pi}{b_2 Z} \left[\frac{r_{1s}^2 - r_{1h}^2}{(r_2 - r_{1s})(1 + \rho_2/\rho_1)} \right] V_{\theta 2} V_{m1} \right\} \quad (5)$$

where ε_c is the clearance gap between the stationary shroud and the rotating blade edges.

Mixing loss

Complicated flow patterns are encountered at the exit from the impeller. Since the flow field has diffused substantially, high aerodynamic blockage is often encountered at the exit. This results in substantial regions of low momentum fluid at the exit and a high energy core. The idea of two-zone flow seems to have been first aired by Dean and Senoo[5] in which the flow was treated as two-dimensional (uniform in the axial direction) with the jet and wake dividing the passage in the circumferential direction. Figure 2 shows the jet and wake flows as presented by Dean and Senoo.

Cumpsty[6] presents the experimental results done by Eckardt[7] to show where the different zones exist (See Figure 3). It can be seen that the wake- or secondary flow exists in the corner where the shroud and the suction side meet.

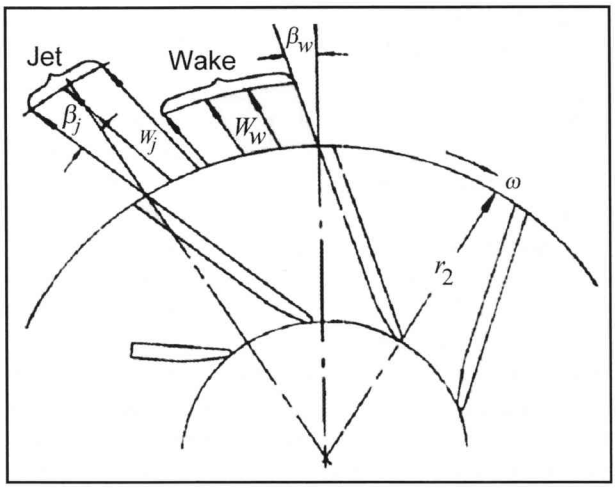

Figure 2: Analytical Model of Impeller Exit Flow. (Taken from Dean and Senoo)

Johnston and Dean[11], as suggested by Oh et al.[4], treat the mixing of the jet and wake flows at the impeller exit (see Figure 2) with a sudden expansion analysis to calculate the mixing loss. They describe how a small control volume is placed across the impeller exit plane and integrated over a given instant of time. This yields the completely mixed out state as one-dimensional flow. They furthermore predict that the radius at which the impeller wakes disappear is very close to r_2 when the jet-wake flow pattern of Dean and Senoo[5] is assumed and when there is no flow in the wakes. The authors state that other studies conducted on instantaneous velocity patterns in typical diffusers support these predictions and that they show even more rapid mixing. The data also suggests that there is very little mass flow in the wakes. Therefore, the sudden mixing process assumed seems to be an authentic model of reality.

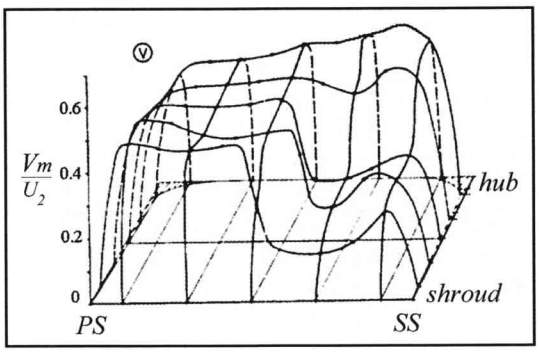

Figure 3: Velocity Distribution at Impeller Exit. (Adapted from Eckardt)

Using conservation of mass, moment of momentum and linear momentum, Johnston and Dean[11] derived equations to calculate the mixing loss. They assumed a square-wave jet-wake relative velocity profile to exit from each blade passage, as done by Dean and Senoo[5], and no variation of relative velocities across the passage depth. In addition they assume that the static pressure is constant around the impeller rim, that the number of blades is large ($z \geq 10$), and that there is no relative flow in the wake. The mixing loss can then be calculated with

$$\Delta h_{mix} = \frac{1}{1 + \tan^2 \alpha_2} \left(\frac{1 - \varepsilon - b^*}{1 - \varepsilon} \right)^2 \frac{V_2^2}{2} \quad (6)$$

where ε is the fraction of the blade-to-blade spacing occupied by the wake (see Figure 2) and b^* is the ratio of the vaneless diffuser inlet depth and the impeller exit depth. This analysis applies only for $b^* \geq 1$, as for $b^* < 1$, an unknown contraction coefficient depending on the detailed shape of the diffuser walls at impeller tip is required. When recast, Equation (6) is identical to the well-known result for the loss of kinetic energy in a one-dimensional sudden expansion.

Ideally one would expect the exit flow to follow the direction of the impeller blades. However, a strong tendency exists for the primary passage flow to migrate from the pressure surface towards the suction surface due to the effect of blade unloading at the airfoil exit. In a centrifugal compressor impeller this is traditionally called slip, as it appears that the flow field has slipped against the direction of rotation from the pressure to the suction side. After the flow has left the impeller, the primary and secondary flows mix, but not ideally, and thus energy is lost and

is referred to as the mixing loss. This process must be understood and modelled accurately if stage performance is to be predicted correctly.

Vaneless diffuser loss

Whether the compressor has a diffuser or not, there is always a vaneless space directly following the impeller where the flow is diffused. It is in this space that the primary and secondary flows mix. As a result of friction and other factors, a loss, referred to as the vaneless diffuser loss, is experienced.

Stanitz[13] developed a numerical procedure for the analysis of flow in a vaneless diffuser. The analysis is for one-dimensional, compressible flow with friction, heat transfer and arbitrary variation in the passage height in vaneless diffusers with arbitrary curvature in the meridional plane. He did not consider the effect of mixing losses. Although the mixing losses are high, this is a favourable approach as mixing losses are already calculated with the loss model described previously. He developed differential equations that relate the change in dependent variables with radius to the design and operating characteristics of the vaneless diffuser. The method makes use of a skin friction factor that is not yet fully understood and does not yet yield satisfactory results. This fact is supported by Japikse[14], but for this study it is not an issue, because it concentrates on the trends rather than the exact magnitude of the losses. According to Cumpsty[6] this one-dimensional approach can be useful to indicate trends.

From the method suggested by Stanitz, Oh et al.[4] subsequently states that the enthalpy loss in the vaneless diffuser to be given by:

$$\Delta h_{vld} = C_p T_{02}\left[\left(\frac{P_3}{P_{03}}\right)^{(\gamma-1)/\gamma} - \left(\frac{P_3}{P_{02}}\right)^{(\gamma-1)/\gamma}\right] \qquad (7)$$

with the loss primarily being caused by the friction between the fluid flow and the surfaces.

Disc friction loss

Disc friction loss occurs as a result of adhesive forces between the rotating disk and the fluid in the surrounding enclosure. The induced flows depend on the geometries of the impeller and its enclosure. Daily and Nece[9] conducted an experimental and theoretical study into the fundamental fluid mechanics with the rotation of a smooth plane disk enclosed within a right-cylindrical chamber. Experimental data was tested against an analysis based on a model recognising all possible flow regimes. The regimes include the combinations of laminar and turbulent flow with merged or separated boundary layers between the rotating disk and stationary wall. Theoretical models were developed for all the different flow regimes. Oh et al.[4] used those models that applied to centrifugal compressors and adopted the following model for enthalpy loss due to disc friction.

$$\Delta h_{df} = f_{df}\frac{\bar{\rho} r_2^2 U_2^3}{4\dot{m}} \qquad (8)$$

Recirculation loss

The flow associated with recirculation is illustrated in Figure 1. It shows how the fluid turns around after leaving the impeller and recirculates back into the impeller section. This will happen more easily when the flow exits the impeller at a large absolute flow angle from the meridional direction. This means, the larger α_2, the more recirculation will take place.

Oh et al.[4] developed a new recirculation loss model by placing more emphasis on the flow angle distribution. In order to connect the loss distribution, they employed a hyperbolic functional form.

$$\Delta h_{rc} = 8\times10^{-5}\sinh\left(3.5\alpha_2^3\right) D_f^2 U_2^2 \qquad (9)$$

Leakage loss

Some of the flow exiting the impeller leaks through the clearance gaps and labyrinth seals to the lower pressure regions of the compressor, causing the leakage loss. The model of Aungier[3] is used to predict the enthalpy loss due to leakage. This includes the disk/housing gap for the disk side and the shroud side for covered impellers and the blade/housing clearance gap for open impellers. The flow in the disk/housing gap is modelled as a forced vortex. This results in the following loss model:

$$\Delta h_{lk} = \frac{\dot{m}_{cl} U_{cl} U_2}{2\dot{m}} \qquad (10)$$

where

$$U_{cl} = 0.816\sqrt{\left(2\Delta P_{cl}/\rho_2\right)} \quad , \quad \Delta P_{cl} = \frac{\dot{m}\left\{r_2 V_{\theta 2} - \left(r_1 V_{\theta 1}\right)_m\right\}}{Z\bar{r}\bar{b}L_\theta}$$

$$\bar{r} = \frac{r_1 + r_2}{2} \quad , \quad \bar{b} = \frac{b_1 + b_2}{2} \quad , \quad \dot{m}_{cl} = \rho_2 Z \varepsilon_c L_\theta U_{cl}$$

Impact of loss mechanisms

The loss models suggested above were programmed into the "Engineering Equation Solver (EES)" software together with a single zone performance prediction method. The purpose was not to verify the loss models, but to perform parametric studies on each of the loss mechanisms to determine the effect of the losses on compressor performance under different operating conditions. It is important to note that this was a qualitative study and not a quantitative study. The important issues here are the trends that the losses exhibit and not the actual values of the different losses.

Incidence loss

The incidence angle is determined by the angle of the relative flow velocity to the blade angle. This means that it can be changed by changing either the rotational speed of the impeller or the mass flow. For the purpose of this study, the mass flow rate was varied.

Figure 4 shows the close to linear relation between the flow angle and the mass flow rate. The difference between the flow angle and the blade angle is the incidence angle. It can be seen that the incidence loss becomes zero where the blade angle and flow angle coincides (around 0.19 kg/s). Furthermore the enthalpy loss is also zero when the incidence angle is zero (where the flow angle and the blade angle coincide) and the incidence loss increases as the absolute incidence angle increases. The larger the incidence angle, the larger the required change in flow direction and therefore the larger the loss. The loss can, however, be minimised through the entire operating range at the cost of installing variable inlet guide vanes to ensure that the flow angle corresponds to the blade angle over most of the operating range. Using the proposed prediction model, the designer can now determine the loss at different operating conditions and determine whether potential improvements justify the cost and complexity of variable inlet guide vanes.

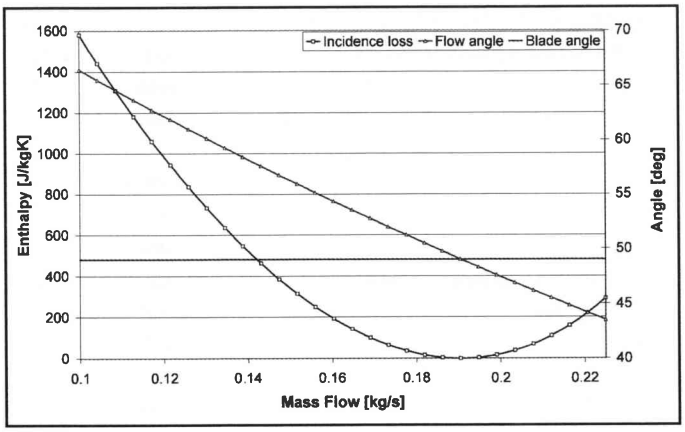

Figure 4: Effect of Mass Flow Change on Flow Angle and Incidence Loss

Blade loading loss

The one-dimensional deceleration of flow component of the diffusion factor (Equation 3) is the ratio of exit relative flow velocity to inlet relative flow velocity at the shroud, W_2/W_{1s}. Increasing the mass flow rate will increase both these velocities. However, the exit relative flow velocity will increase at a higher rate than that of the inlet relative velocity at the shroud because of the greater tangential impeller speed at the exit ($U_2 > U_{1s}$), which is a typical characteristic of the centrifugal compressor.

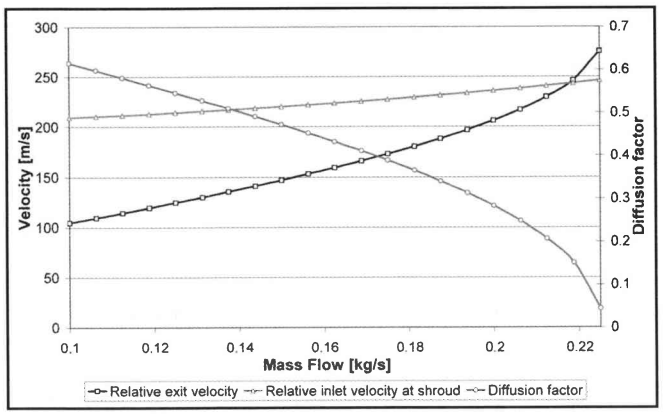

Figure 5: Effect of Mass Flow Change on Relative Velocities and Diffusion Factor

From Figure 5 it can be seen that the diffusion factor D_f reduces as the speed increases. This decrease in the diffusion factor causes a reduction in the blade loading loss. This means that the loss of momentum due to boundary-layer build-up on the blade surfaces will decrease as the momentum of the fluid increases due to higher relative flow velocities. Figure 6 illustrates the decrease in blade loading loss due to the reduction in diffusion factor. Based on the above it can be deducted that the loss is reduced by increasing the relative flow velocity and that this can be achieved by either increasing the impeller rotational speed or the axial velocity (i.e. mass flow) or both.

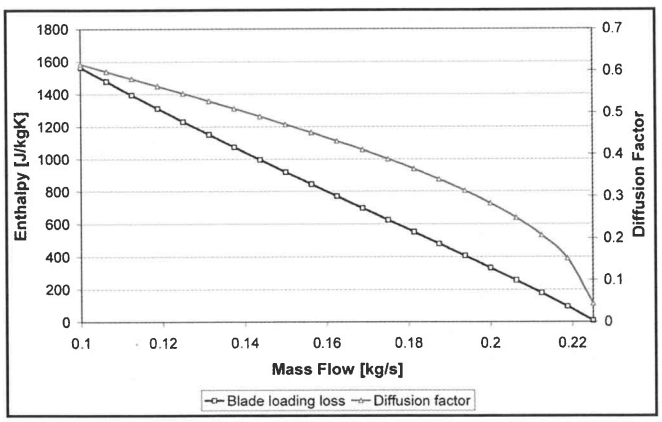

Figure 6: Effect of Mass Flow Change on Blade Loading Loss and Diffusion Factor

Skin friction loss

From Equation (4) it can be seen that the loss will increase as the flow velocity increases. This is confirmed by Figure 7 illustrating how the loss increases with an increase in mass flow rate, which in turn increases the mean velocity component.

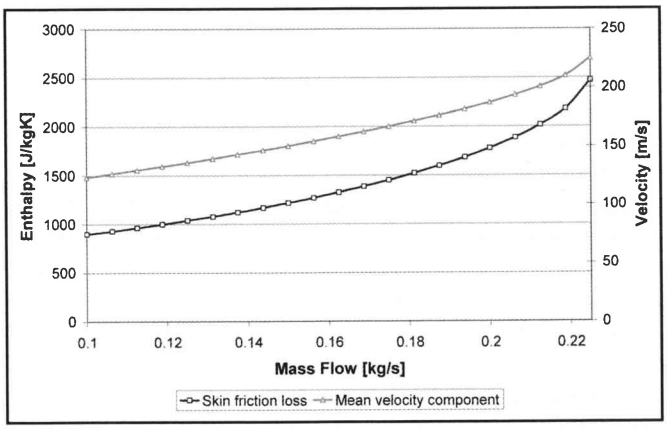

Figure 7: Effect of Mass Flow Change on Skin Friction Loss and Velocity

The skin friction loss is also directly dependent on the friction factor. Using the model for skin friction loss, the designer can calculate the exact magnitude of the loss effect on efficiency to determine whether the additional machining cost to obtain a smoother blade surface is justifiable or not.

Clearance loss

The larger the gap between the blade and the housing, the larger the leakage flow and associated loss that can be expected due to the pressure difference over the blades. The loss is also increased by a larger difference in velocity between the main flow and the leakage flow. Increasing the mass flow increases the flow velocity through the impeller. This causes the difference in velocity between the leakage flow and the main flow to increase, thus increasing the clearance loss. However, at some stage the clearance loss starts to decrease although the mass flow still increases (see Figure 8). This can be explained by the fact that

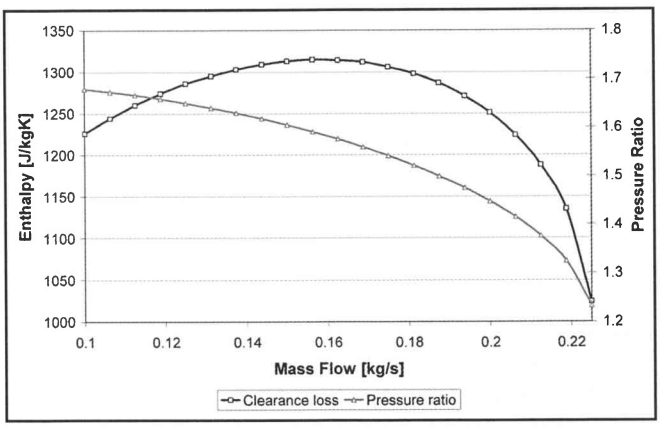

Figure 8: Effect of Mass Flow Change on Clearance Loss and Pressure Ratio

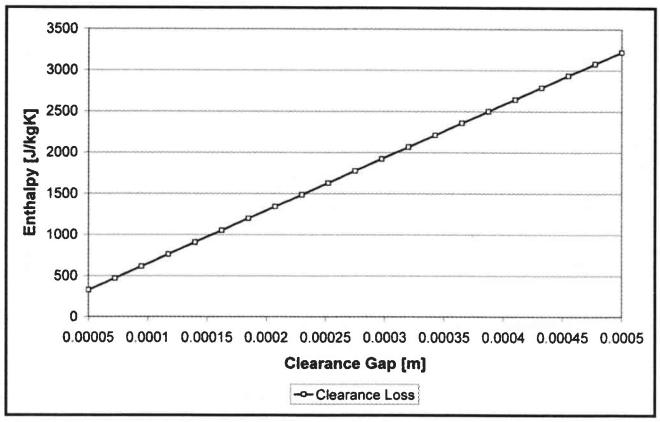

Figure 9: Effect of Clearance Gap Change on Clearance Loss

the pressure ratio decreases as a result of increasing mass flow, a characteristic of compressor performance curves. The lower pressure ratio causes less flow to leak over the impeller blades, thus decreasing the clearance loss.

Increasing the clearance gap causes more fluid to leak over the impeller blades and cause greater mixing of the flows, increasing the clearance loss. Figure 9 subsequently confirms the clearance loss to increase linearly with an increase in the clearance gap.

From the above mentioned it is important to keep the clearance gap as small as possible. However, this impacts rather severely on the manufacturing tolerances making it a rather expensive process for high performance designs. Using the model for clearance loss, the designer can now calculate the clearance loss and optimise performance with respect to minimising clearance loss and unit cost.

Mixing loss

Examining Equation (6), it is clear that the mixing loss is directly dependent on the magnitude of the wake flow, which is a function of the fraction of wake flow area ε. This means that the larger the wake flow fraction, the more mixing will take place between the jet and wake flows and therefore the larger the mixing loss will be. It is therefore important to use accurate values for ε.

The different ways to model the mixing loss is firstly to assume a constant ε and secondly to vary ε with a change in operating conditions. In both cases it is complicated to determine accurate values for ε. In the study performed by Johnston and Dean[11] they clearly state that the prediction of ε was "intentionally ignored" because it depends upon the detailed internal flow mechanisms of the impeller. These include the location of the separation lines in the blading, hub and shroud, which in turn depend upon the aerodynamic loading of these surfaces, flow Reynolds and Mach numbers, rotational effects, etc. For the purpose of this study a correlation will therefore be used for the values of ε.

Oh et al.[12] suggests that the wake mass flow fraction (χ) varies between 0.15 and 0.25. Using these values in an equation provided by Oh et al. to calculate the variation of the wake flow fraction with flow rate, $\chi = 0.93\varepsilon^2 + 0.07\varepsilon$ yields values for ε of 0.366 to 0.482.

For the first method a constant value of 0.4 was assumed for ε and the results are shown in Figure 10. It is clear that the mixing loss increases with an increase in mass flow rate. The problem with these results is that Whitfield and Baines[2] state that the jet flow area increases with increasing mass flow rate. This means that the wake flow area is decreasing and the mixing loss should decrease with an increasing mass flow rate. This is not the case in Figure 10, which raises the question whether the choice of a constant ε is acceptable.

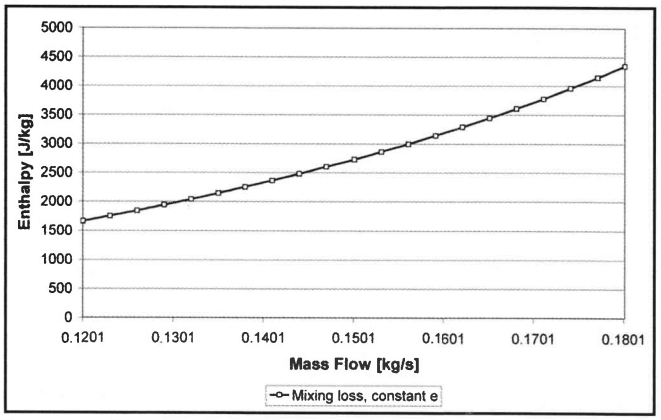

Figure 10: Effect of Mass Flow Change on Mixing Loss with Constant ε

Figure 11 illustrates the mixing loss with a change in mass flow rate and with the values of ε ranging from 0.5 at the low mass flow to 0.366 at the higher mass flow. The higher value of 0.5 was used instead of 0.482 because 0.482 showed a small increase in mixing loss at the lower mass flow region. These results illustrate a more realistic simulation of the mixing loss.

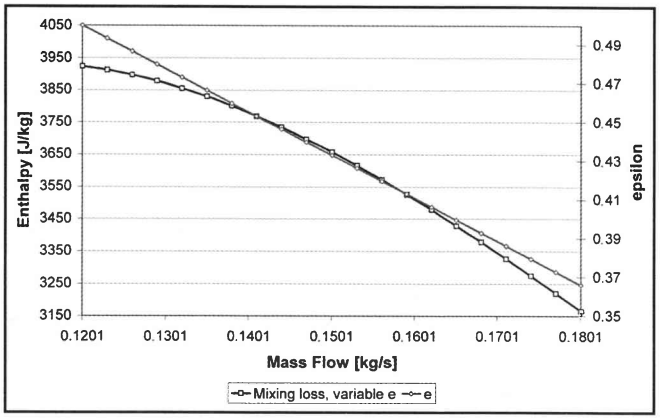

Figure 11: Effect of Mass Flow Change on Mixing Loss with Variable ε

Based on the above it therefore seems incorrect to assume a constant value for ε. The uncertainty surrounding the exact influence of the wake flow requires more research to either confirm or improve the existing models.

Vaneless diffuser loss

The loss in the vaneless diffuser is caused by the friction between the fluid flow and the surfaces of the flow passage. This means that the higher the flow velocity or the longer the flow surfaces, the higher the loss. However, the increase in the radius only increases the flow length while the velocity reduces due to the increased diffusion (larger flow area).

Figure 12 shows the increase in vaneless diffuser loss due to increased diffuser exit radius while Figure 13 shows the effect of an increased mass flow.

The effective flow length is determined by the absolute flow angle in the diffuser. The flow follows a spiral flow path through the diffuser and therefore the higher the absolute flow angle at

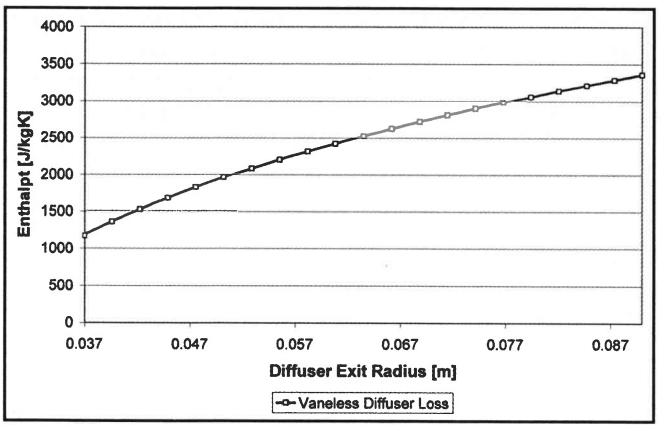

Figure 12: Effect of Diffuser Exit Radius on Vaneless Diffuser Loss

the exit of the impeller, the longer the effective flow path will be. As shown in Figure 13, the velocity decreases to a minimum and then increases sharply. It is expected that the loss should follow the behaviour of the velocity, but the loss curve lags behind the velocity curve. However, the absolute flow angle at the impeller exit (α_2) decreases at a constant rate from 71° to 45° over the mass flow range (not shown). Thus, the lag in the vaneless diffuser loss can be attributed to the shortening of the effective flow length. The combination of a small increase in velocity and decreasing effective flow length at $\dot{m}$ <0.16 keeps decreasing the loss, but at $\dot{m}$ >0.16 the sharp increase in velocity dominates and the loss starts to increase.

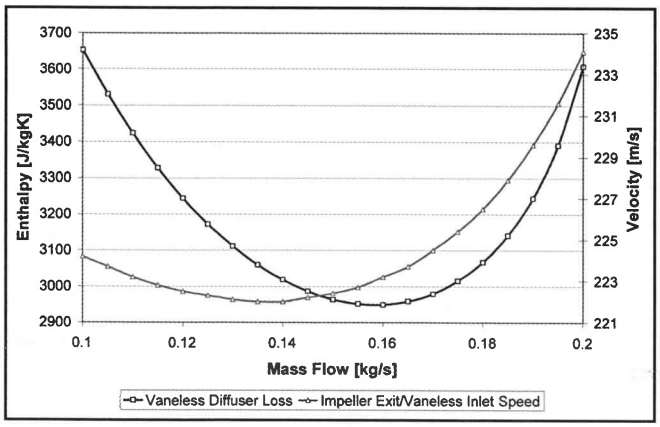

Figure 13: Effect of Velocity Change on Vaneless Diffuser Loss

The losses are low around the design point due to the exit flow having a favourable ratio of velocity and flow path length. Minimising these parameters would minimise the loss. Well designed vaned diffusers can aid in this, but at the cost of a more expensive diffuser.

Disc friction loss

Disc friction loss is influenced by the friction between a fluid and a rotating disc. Although not quite the same, it is closely related to skin friction loss and is affected by the difference in speed between the disc and fluid as well as the size of the contact area (determined by the exit radius).

From Equation (8) it can be expected that a higher rotating disk speed (larger difference between surface speed and fluid velocity) or larger contact area will increase the loss. The results obtained from simulations confirmed this as can be seen from Figure 14 and Figure 15 respectively. When choosing the impeller dimensions and rotating speed, the designer has to

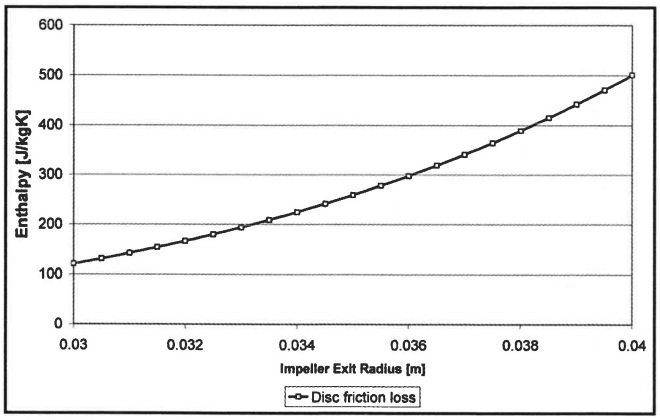

Figure 14: Effect of Rotational Speed on Disc Friction Loss

weigh the increased pressure ratio due to these effects against the increased losses (or reduced efficiency) that will be experienced.

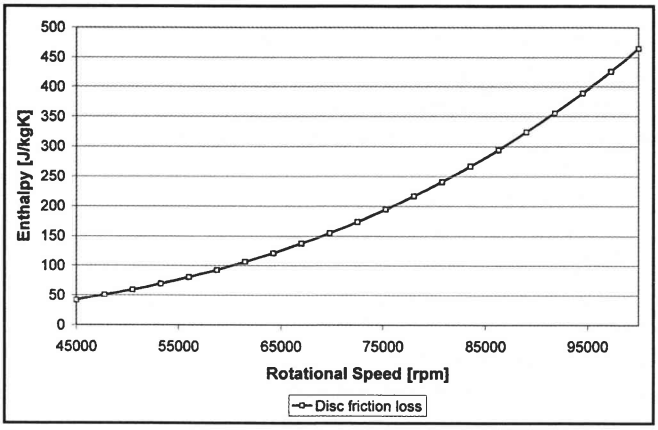

Figure 15: Effect of Impeller Exit Radius on Disc Friction Loss

Recirculation loss

A parametric study was done to determine which changes in the various variables would have the greatest effect on the recirculation loss (see Figure 1). For the purpose of this paper only the effect of the mass flow rate and the rotational speed of the compressor will be addressed.

Figure 16 illustrates the decrease in absolute exit flow angle with an increase in mass flow rate. This decreases the tendency to recirculation thus decreasing the recirculation loss. The rather high recirculation loss in the extreme low mass flow range (0.05 to 0.06 kg/s) can be attributed to the large absolute exit flow angle being excessive (close to 80°).

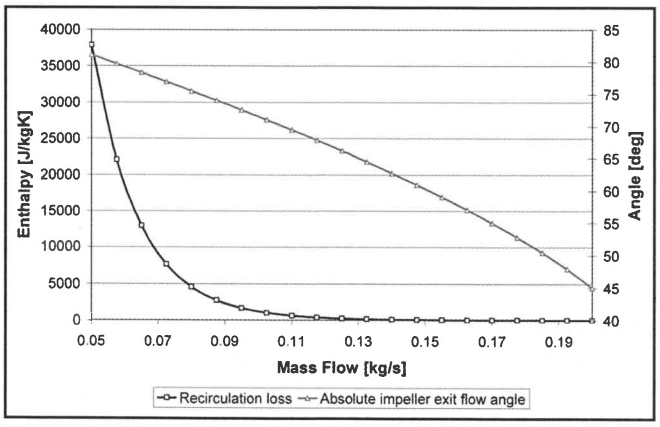

Figure 16: Effect of Mass Flow Change on Recirculation Loss

Figure 17 illustrates the increase of the tangential impeller exit speed with an increase in rotational speed. This causes the absolute impeller exit angle to increase, thus increasing the tendency for recirculation and the associated loss. Once again excessive flow angles are experienced at high impeller speeds resulting in a sharp increase in the recirculation loss.

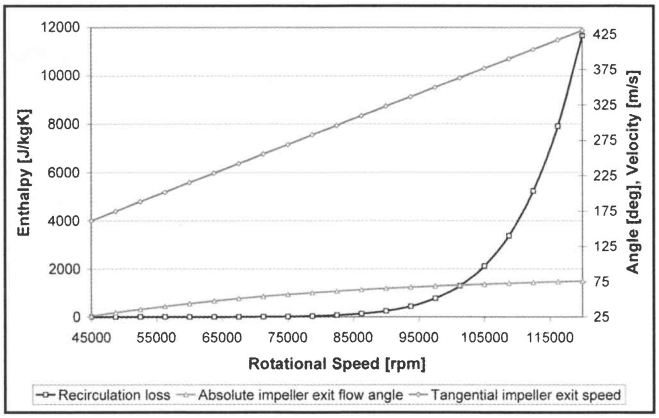

Figure 17: Effect of Rotational Speed on Recirculation Loss

From the above it can be stated that care should be taken when designing the impeller or choosing the operating speed to ensure optimum operation at the intended mass flow and lowest possible recirculation loss.

Leakage loss

Figure 1 shows how the flow exiting the impeller at high pressure leaks through small gaps to regions of lower pressure. The model for leakage loss presented by [3] calculates the pressure difference over the leakage areas and the leakage mass flows through the areas. Evaluating this realistically, the leakage loss will be higher if the leakage mass flow or the pressure difference is larger. The larger the clearance gap, the easier the fluid can flow through it, resulting in an increased leakage loss (see Figure 18). This means that in order to limit leakage loss, the clearance gap should be kept to a minimum. However, this comes with a cost penalty which the designer has to consider when specifying the required clearance gap.

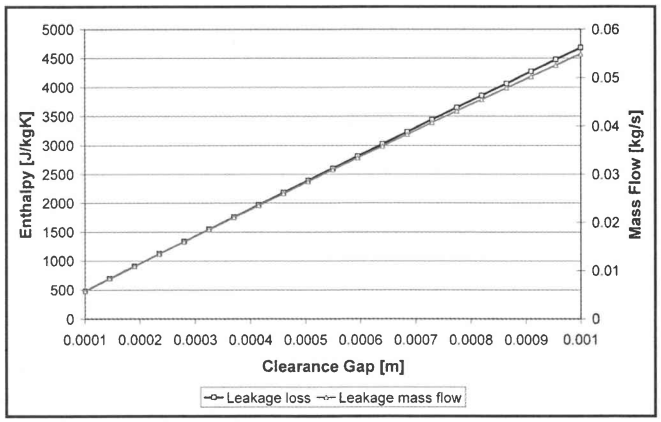

Figure 18: Effect of Clearance Gap on Leakage Loss and Leakage Mass Flow

Loss distribution

With the loss mechanisms being studied individually, the designer can now use some or all the loss models to aid in the designing process. However, in order to have the largest possible effect on performance at the lowest possible cost it is important to identify the losses to focus on during the design process.

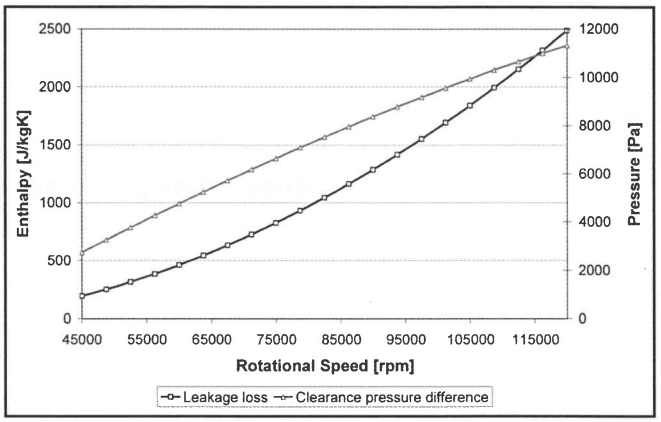

Figure 19: Effect of Rotational Speed on Leakage Loss and Leakage Pressure Difference

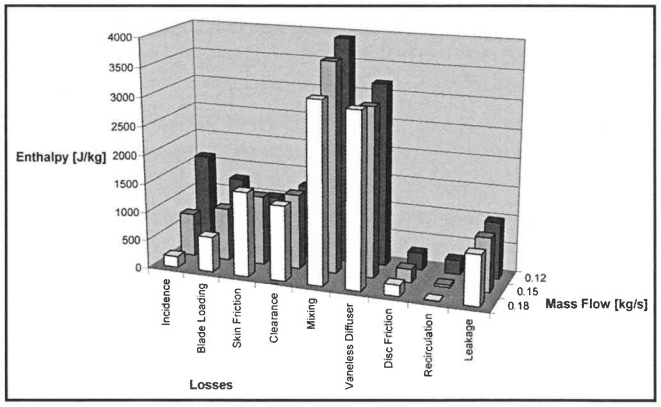

Figure 20: Loss Distribution

Figure 20 subsequently shows the loss distribution over a typical mass flow range. It shows that the losses follow the same characteristic as in the preceding paragraphs with the mixing and the vaneless diffuser losses dominating the internal losses. Furthermore, the mixing loss is a characteristic of the centrifugal compressor and will always be one of the dominant losses. However, further studies should be done to determine more accurate values for the wake fraction to improve the accuracy of the mixing loss prediction. The vaneless diffuser loss can be minimised by decreasing the length of the vaneless diffuser, but at a cost of pressure recovery. It is thus up to the designer to calculate an optimum length for the vaneless diffuser.

Figure 21 furthermore illustrates the pressure ratio and the efficiency over the mass flow range. It is clear that the lower

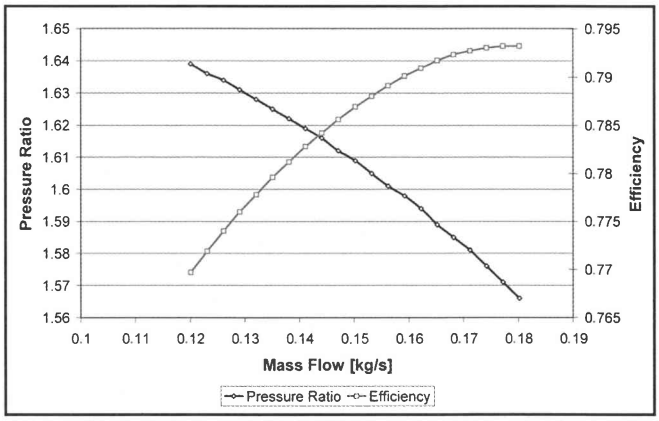

Figure 21: Pressure Ratio and Efficiency

parasitic losses at higher mass flow rate increases the efficiency significantly. It therefore supports the suggestion to focus on reducing the losses in order to improve performance.

Conclusion

This study investigated the effect of loss mechanisms and loss distributions of centrifugal compressors to aid in the designing process. Using the foregoing discussions in the design process can help to eliminate trial-and-error type designing and optimise the design faster and more efficiently. The designer can use these loss models to justify certain costly design optimisations by identifying the trend of a certain loss mechanism and applying that knowledge in the design.

With the loss mechanisms having been studied individually, the designer can use some or all the loss models to aid in the design process. However, it also offers the potential to identify the most important losses to focus on in order to improve performance with the least impact on cost.

References

1. Jansen, W. 1967. A method for calculating the flow in a centrifugal impeller when entropy gradients are present. *Institution of Mechanical Engineers, Royal Society Conference on Internal Aerodynamics (Turbomachinery):133-146, Jul. 19.*

2. Whitfield, A., Baines, N.C. 1990. Design of radial turbomachines. *Harlow Essex:Longman Scientific & Technical. 397 p.*

3. Aungier, R.H. 1995. Mean streamline aerodynamic performance analysis of centrifugal compressors. *Transaction of the ASME. Journal of Turbomachinery, 117(3):60-366, Jul. 31.*

4. Oh, H.w., Yoon, E.S., Chung, M.K. 1997. An optimum set of loss models for the performance prediction of centrifugal compressors. *Proceedings of the Institution Mechanical Engineers. Journal of Power and Energy, 211(A4):331-338.*

5. DeanJr. R.C., Senoo, Y. 1960. Rotating wakes in vaneless diffusers. *Transaction of the ASME. Journal of Basic Engineering, 82:563-574, Sep.*

[6]CUMPSTY , N.A. 1989. Compressor Aerodynamics. *1st ed. Essex:Longman Scientific & Technical. 509 p.*

7. Eckardt, D. 1976. Detailed flow investigations within a high speed centrifugal compressor impeller. *Transaction of the ASME. Journal of Fluids Engineering 98:390-402, Sep.*

8. Japikse, D., Baines, N.C. 1997. Introduction to Turbomachinery. *2nd ed. Concepts ETI, USA:Edwards Brothers Incorporated. 11-59 p.*

9. Daily, J.W., Nece, R.E. 1960. Chamber dimension effects on induced flow and frictional resistance of enclosed rotating disks. *Transaction of the ASME. Journal of Basic Engineering, 82:217-232, Mar.*

10. Conrad, O., Raif, K., Wessels, M. 1980. The calculation of performance maps for centrifugal compressors with vane-island diffusers. *In ASME Twenty-fifth Annual International Gas Turbine Conference and Twenty-second Annual Engineering Conference on Performance Prediction of Centrifugal Pumps and Compressors. New Orleans, Louisiana :135-147, Mar.*

11. Johnston, J.P., Dean Jr, R.C. 1966. Losses in vaneless diffusers of centrifugal compressors and pumps. Analysis, experiments, and design. *Transaction of the ASME. Journal of Engineering for Power, 88:49-62.*

12. hH, H.W., Yoon, E.S., Chung, M.K. 2002. Systematic two-zone modelling for performance prediction of centrifugal compressors. *Proceedings of the Institution Mechanical Engineers. Journal of Power and Energy, 216(A):75-87.*

13. Stanitz, J.D. 1952. One-dimensional compressible flow in vaneless diffusers of radial- and mixed-flow centrifugal compressors, including effects of friction, heat transfer and area change. *National Advisory Committee for Aeronautics. Technical note 2610. Jan.*

14. Japikse, D., 2004. Optimisation in turbomachinery data reduction. *10th International Symposium on Transport Phenomena and Dynamics of Rotating Machinery (ISROMAC-10) Honolulu, Hawaii. Mar.*